UNCLASSIFIED
SECURITY CLASSIFICATION OF THIS PAGE

REPORT DOCUMENTATION PAGE

Form Approved
OMB No 0704-0188

AD-A212 689

1b RESTRICTIVE MARKINGS

DTIC FILE COPY

3 DISTRIBUTION/AVAILABILITY OF REPORT
This document has been approved for public release and sale; its distribution is unlimited.

4 PERFORMING ORGANIZATION REPORT NUMBER(S)
IBM Research Report RJ7015

5 MONITORING ORGANIZATION REPORT NUMBER(S)
Technical Report #20

6a NAME OF PERFORMING ORGANIZATION
IBM Research Division
Almaden Research Center

6b OFFICE SYMBOL (If applicable)

7a NAME OF MONITORING ORGANIZATION
Office of Naval Research

6c ADDRESS (City, State, and ZIP Code)
650 Harry Road
San Jose, CA 95120-6099

7b ADDRESS (City, State, and ZIP Code)
Chemistry Division Code 1113
Arlington, VA 22217

8a NAME OF FUNDING/SPONSORING ORGANIZATION
Office of Naval Research

8b OFFICE SYMBOL (If applicable)

9 PROCUREMENT INSTRUMENT IDENTIFICATION NUMBER
N00014-84-C-0708, 4131022

8c ADDRESS (City, State, and ZIP Code)
Chemistry Division, Code 1113
Arlington, VA 22217

10 SOURCE OF FUNDING NUMBERS

PROGRAM ELEMENT NO	PROJECT NO	TASK NO	WORK UNIT ACCESSION NO

11 TITLE (Include Security Classification)
Photon-Gated Persistent Spectral Hole-Burning

12 PERSONAL AUTHOR(S)
W.E. Moerner

13a TYPE OF REPORT	13b TIME COVERED	14 DATE OF REPORT (Year, Month, Day)	15 PAGE COUNT
Interim Technical	FROM _____ TO _____	1989, September 11	27

16 SUPPLEMENTARY NOTATION
Submitted for publication in Japanese Journal of Applied Physics

17 COSATI CODES			18 SUBJECT TERMS (Continue on reverse if necessary and identify by block number)
FIELD	GROUP	SUB-GROUP	Photon-Gating Persistent Spectral Hole-Burning Frequency Domain Optical Storage

19 ABSTRACT (Continue on reverse if necessary and identify by block number)

This article reviews recent progress in the area of photon-gated persistent spectral hole-burning, in which one photon selects absorbers in an inhomogeneously broadened line and a second "gating" photon of a different wavelength completes the excitation necessary to produce a spectral hole. This phenomenon provides a crucial threshold in the hole formation process, allowing reading with the first wavelength alone to be nondestructive. Examples of photon-gating in both inorganic and organic materials are summarized, with emphasis on the organic materials.

20 DISTRIBUTION/AVAILABILITY OF ABSTRACT
☒ UNCLASSIFIED/UNLIMITED ☐ SAME AS RPT ☐ DTIC USERS

21 ABSTRACT SECURITY CLASSIFICATION
UNCLASSIFIED

22a NAME OF RESPONSIBLE INDIVIDUAL
Dr. W.E. Moerner

22b TELEPHONE (Include Area Code)
(408) 927-2426

22c OFFICE SYMBOL

DD Form 1473, JUN 86 Previous editions are obsolete S/N 0102-LF-014-6603

SECURITY CLASSIFICATION OF THIS PAGE
UNCLASSIFIED

89 9 20 103

OFFICE OF NAVAL RESEARCH

Contract N00014-84-C-0708

R&T Code 4131022

Technical Report No. 20

Photon-Gated Persistent Spectral Hole-Burning

by

W. E. Moerner

Prepared for Publication

in

Japanese Journal of Applied Physics

IBM Research Division
Almaden Research Center
650 Harry Road
San Jose, California 95120-6099

September 11, 1989

PHOTON-GATED PERSISTENT SPECTRAL HOLE-BURNING

W. E. Moerner

IBM Research Division

Almaden Research Center

650 Harry Road

San Jose, California 95120

ABSTRACT: This article reviews recent progress in the area of photon-gated persistent spectral hole-burning, in which one photon selects absorbers in an inhomogeneously broadened line and a second "gating" photon of a different wavelength completes the excitation necessary to produce a spectral hole. This phenomenon provides a crucial threshold in the hole formation process, allowing reading with the first wavelength alone to be nondestructive. Examples of photon-gating in both inorganic and organic materials are summarized, with emphasis on the organic materials.

§1. Introduction

Frequency domain optical storage, in which digital information is encoded as the frequency location of persistent spectral holes,[1] shows promise of high areal densities in the $10^9 - 10^{11}$ bits/cm^2 range while affording fast random access by beam deflection as well as high data rates by laser frequency tuning and optical parallelism. Persistent spectral hole-burning (PSHB) occurs in inhomogeneously broadened optical transitions of impurities in transparent solids at low temperatures when optical excitation of resonant impurity centers causes a long-lived transformation to a new nonabsorbing ground state. In addition to the interest in PSHB for possible storage applications[2], this phenomenon has proven to be extremely useful in the study of the statics and dynamics of absorbing centers in a wide variety of amorphous and crystalline solids[3].

A material in order to be useful in a practical frequency-domain optical storage system must simultaneously show the ability to form deep holes in short (nanosecond) burning times and yet allow nanosecond reading at high signal-to-noise ratios with tightly focused beams. These requirements place several well-defined constraints on the dynamical properties of the hole-burning mechanism. For the case of single-photon materials in which the photoinduced change proceeds with a certain fixed probability after the absorption of one photon by each absorbing center, a thorough analysis of the coupled reading-writing problem[4] shows that these materials can provide sufficient SNR only in a limited range of absorption cross sections and quantum efficiencies. The essential problem with single-photon processes is that there is no threshold or hysteresis in the hole formation mechanism, as opposed to the situation with all other successful schemes for long-term information storage such as magnetic, magneto-optic, ferroelectric, and phase change recording.

One way around the destructive reading problem with single-photon materials is to consider two-step spectral hole formation mechanisms, called gated mechanisms (see Fig. 1).

A gated mechanism has the property that irradiation with the wavelength λ_1 alone causes essentially no photoinduced changes (writing), i. e., after the absorption event takes the center from the ground state 1 to the excited state 2, the center simply returns to the original ground state 1 after the excited state lifetime. However, when the center has been placed in the excited state 2 by absorption of a photon at λ_1 *and* an external "gating field" is also present, a photoinduced change occurs and the center enters a new ground state or permanent reservoir that no longer absorbs at λ_1. The "dip" or region of reduced absorption that is left behind in the inhomogeneous line is the resulting spectral hole that can be detected nondestructively with λ_1 alone. In this manner, gated mechanisms add a crucial threshold to the hole formation process, which allows the writing and reading processes to be uncoupled. The external field may be a second photon of a different wavelength or the gating could perhaps be achieved by any other external field, such as electric field, magnetic field, stress field, and the like. When the gating field is a second light field[5], the mechanism is said to be *photon-gated.*

The importance of photon-gated processes for scientific studies of PSHB and for frequency domain optical storage has stimulated much recent research to discover new photon-gated materials. This paper will first present schematic energy level schemes for photon-gating appropriate for 3-level and 4-level systems (§2). In most cases, the mechanism is two-step photoionization, although other biphotonic photochemical reactions have also produced photon-gating (see §3.2). In §3, recent progress in the search for photon-gated systems in inorganic materials as well as in organic materials will be briefly reviewed. Some emphasis will be placed on the organic materials since a review of the inorganic materials has appeared recently[6]. This work concludes (§4) with a description of the optimal cross section, quantum efficiency, and number density for an optimal photon-gated material for the case of frequency domain readout in focused spots.

§2. Generalized Photon-Gated Mechanisms

Figure 2 illustrates some general requirements on three-level and four-level photon-gated PSHB mechanisms in order to achieve high overall efficiency and high gating ratio, where the gating ratio is a measure of the efficiency of two-color hole production divided by the efficiency of one-color hole production with λ_1 alone. While the exact materials requirements depend strongly upon the actual system configuration and signal-to-noise requirements, some general comments about the required level structure can be made.

The left side of Fig. 2 illustrates the three-level system which is the common configuration for many inorganic materials. A first requirement is that λ_1 should be larger than λ_2, so that the site-selecting beam cannot also easily act as the gating beam. The absorption in the circular regions should be small to reduce one-color burning (by three λ_1 photons, case a) or bleaching by the gating light (by two λ_2 photons, case b). The lifetime τ of the intermediate state 2 should be long enough to allow large populations to build up in this state for further excitation to the reactive levels 3. In cases where τ is much larger than the data access time the storage material does not have to be exposed to both photon energies simultaneously. Further, there is no fundamental need for a frequency-selective narrow-band transition from level 2 to level 3; however, in certain instances, narrow-band levels 3 involving transitions with high peak cross sections may be preferable to a continuum absorption such as a conduction band. The microscopic yield η from the reactive levels 3 should be as large as possible for high overall gating efficiency.

In principle, systems with $\lambda_1 = \lambda_2$ can exhibit gated PSHB in the sense that the hole-burning yield is nonlinear with laser intensity[7]. For example, at low powers the hole formation rate may scale quadratically with laser power, whereas at high powers level 2 saturates and the hole formation rate scales linearly with laser power. However, in actual situations, signal-to-noise requirements often require that the reading laser power be so large that the quadratic regime cannot be utilized. In addition, the requirement of non-destructive

reading makes it desirable to use systems with $\lambda_1 \neq \lambda_2$ permitting complete decoupling of reading and writing processes.

The right half of Fig. 2 illustrates optimized photon-gated PSHB with a four-level system. Here the intermediate state i is distinct from state 2, which allows independent optimization of the level lifetimes. This level structure occurs quite commonly for organic materials in which states 1 and 2 are part of the singlet manifold and level i is the lowest triplet state. The required lifetime τ of level 2 will often be determined by a combination of the required hole width, data rate, and absorption strength. For example, if τ is too short, the holes will be necessarily broad. For efficient gated PSHB the ($2 \rightarrow i$) rate Γ_i should be as large as possible consistent with the requirement that the lifetime of level 2 not be too short. Further, a long intermediate state lifetime τ_i would be advantageous in achieving a large population in level i. It is evident that absorptions $2 \rightarrow$ (a), $1 \rightarrow$ (b), and $i \rightarrow$ (c) involving photons of frequency ω_1, ω_2, and ω_1, respectively, should not be large in order to prevent undesired bleaching and inefficient excitation of interfering levels. Of course, the microscopic yield η from the photoreactive levels 3 should be as large as possible for efficient photon-gating.

§3. Examples of Photon-Gating

§3.1 *Inorganic Materials*

The first observation of photon-gating resulted from experiments on Sm^{2+} ions in BaClF crystals [8]. This material is in the class of 3-level materials (Fig. 2, left side), and the specific energy levels of interest are shown in Figure 3. Despite the discovery of several other inorganic systems showing photon-gating, this material continues to be of interest due to the large gating ratio and other properties to be described below. The first photon near 690 nm excites the system from the $^7F_0$ ground state (level 1) to the $^5D_0$ level (level 2). Extended irradiation at 690 nm produces essentially no hole production, but brief periods of simultaneous irradiation with $\lambda_2 = 514$ nm or shorter produces spectral holes at λ_1. The

second photon excites the ion from $^5D_0$ to the conduction band or to an autoionizing level above the conduction band edge and the liberated electron is subsequently trapped in the host matrix leaving behind a Sm^{3+} ion.

Figure 4 shows examples of the spectral holes for the Sm^{2+}:BaClF system. The gating ratio, or the ratio of gated hole depth to single-color hole depth for equal λ_1 burning conditions, has been observed to be quite large, on the order of 10^4. Another novel property of this system is room temperature cyclability of the written information[9]. For example, after burning holes at liquid helium temperatures, the sample can be warmed up to room temperature for 24 hours, and then upon recooling to helium temperature, the previously written holes can still be easily detected.

Since the hole-burning process appears to involve conversion of Sm^{2+} to Sm^{3+} with trapping of the ejected electron at Sm^{3+} ions, the act of hole-burning simply redistributes absorption strength within the inhomogeneous absorption of the Sm^{2+} ions. The holes can be erased by irradiation in the homogeneously broadened transitions in the blue, which redistributes the ions between the divalent and trivalent states. One drawback of this material, however, is the extremely small oscillator strength of the λ_1 transition, which makes high SNR experiments in thin films difficult.

Table 1 lists the inorganic photon-gated materials studied to date. For full detail, the reader is encouraged to consult the references. As can be seen, the divalent Sm ion shows gating in a number of host crystals. In addition, the transition from the ground state to the $^5D_1$ state shows photon-gating[10]. Recently, using a mixed crystal of BaClF and BaBrF to increase the inhomogeneous broadening, photon gating was observed at 77K by Wei, et al.[12].

One possible approach to higher absorption cross sections in the inorganics lies in the study of multivalent transition metal ions in crystals (see the last two entries in Table 1). For example, Co^{2+} in an inverse spinel crystal, $LiGa_5O_8$ has shown photon-gating[13]. This inorganic material utilizes 660 nm for λ_1 and longer wavelengths for λ_2 leading to a gating

ratio of $\simeq$ 20. The mechanism is similar to that for the Sm^{2+}:BaClF material: two-step photoionization and trapping of the ejected electron in the host crystal. Cr^{3+} in $SrTiO_3$ has also shown photon-gating[6], but with a reduced gating ratio.

§3.2. *Organic Materials*

Spectral hole-burning nonlinear in the burning intensity was observed quite early in the history of hole-burning (see Ref. 7 for details), but the importance of photon-gating with two-color excitation was not realized until much later, after the SNR analysis of single-photon materials[4]. Table 2 lists organic materials showing two-color photon-gated PSHB to date. In these materials, the 1→2 transition is usually within the singlet-singlet manifold, thus the absorption cross section is often quite large. Optical densities of 0.3 or more are relatively easy to achieve in thin films. The level scheme most often applicable to these systems is shown in the right half of Fig. 2.

The first example of two-color photon-gated PSHB in organic materials was provided by carbazole molecules in boric acid glass [15]. Upon excitation in the singlet-singlet origin with $\lambda_1 = 335$ nm, the molecule undergoes intersystem crossing with a high yield to build up a large metastable population in the lowest triplet state, T_1. In the presence of $\lambda_2 = 360 - 514$ nm, holes are formed at the singlet excitation wavelength, λ_1, due to photoionization of the molecule in the triplet manifold and trapping of the ejected electron in the boric acid glass matrix. The observed gating ratio for this material is near 400. The boric acid glass matrix plays an important role: in comparison to less polar hosts like PMMA, boric acid glass lowers the ionization potential of the carbazole guest from the gas phase value by 2.3 eV. The difficulty with this material is the short wavelength of the site-selecting transition: λ_1 alone is sufficient to cause photoionization via a biphotonic process.

The group of Korotaev, et al., reported two-color hole-burning for a derivative of Zn-tetrabenzoporphyrin in uncharacterized PMMA[16] with excitation at 628 and 337 nm.

The mechanism was not determined, and the authors felt that a photoionization process was unlikely in this system.

The organic material composed of photoadducts of anthracene and tetracene (A-T) in PMMA [17] provides a quite different type of photoreaction leading to photon-gating: two-step photodissociation of the adduct. The gating ratio for this material is small, however, due to one-color photoreactions caused by the absorption of two photons of $\lambda_1 = 326$ nm. The one-color and two-color hole-burning kinetics for this system show both transient and photochemical saturation effects [18].

Studies of the molecule TZT (meso-tetra-(p-tolyl)-Zn-tetrabenzoporphyrin) in ultrapure primary standard PMMA using toluene as a solvent yielded only single-photon photophysical hole-burning[19]. However, by utilizing halomethane solvents, photon-gating was observed by a particularly interesting mechanism: donor-acceptor electron transfer from the excited porphyrin donor to a nearby halomethane acceptor[19]. The TZT donor (or its Mg analog) was found to exhibit photon gating in well-characterized PMMA thin films in the presence of a variety of halomethane acceptors, such as chloroform ($CHCl_3$), methylene chloride, or methylene bromide [20]. The schematic mechanism for hole production is shown in Fig. 5. The frequency selecting photon $\lambda_1 \simeq 630$ nm excites the lowest singlet-singlet transition, and triplets are produced efficiently by virtue of the high triplet yield (0.8). The triplet lifetime of 40 ms (for the Zn compound) facilitates the buildup of a large population in T_1. When the gating light at $\lambda_2 = 350 - 800$ nm is present, the electron is excited to an upper triplet T_n from which it tunnels to a nearby halomethane acceptor. This mechanism has been confirmed by time-delayed two-color hole burning and measurements of the spectrum of the porphyrin cation photoproduct[20].

This first example of photon-gating via a clearly defined donor-acceptor electron transfer mechanism has the useful property of allowing the gating effect to be controlled by varying the acceptor concentration and/or acceptor electron affinity (by choosing a different acceptor). However, due to subsequent reaction of the reduced acceptor with the matrix,

reversal of the electron transfer is somewhat difficult. This lack of reversibility is not a fundamental problem because one can envision directly coupled donor-acceptor molecules in which the electron can be reversibly shuffled back and forth between the two halves of the molecule in a fashion analogous to the proton tautomerization reaction for the free-base porphyrins and phthalocyanines.

Aside from the specific disadvantage of irreversibility, the TZT $CHCl_3$ PMMA material and its analogs with Mg and with other halomethanes have a further useful property: the overall efficiency of gated hole production is high: i.e., fairly deep ($\sim$ 1"% in transmission) holes can be burned with a *single* 8 ns pulse at λ_1 followed immediately by a 200 ms gating pulse at λ_2[21]. This is a result of several factors: the large absorption cross section at λ_1, the large triplet yield, the reasonably long triplet lifetime, and the large intrinsic probability for electron transfer from the high triplet levels to the nearby acceptor.

Figure 6 illustrates a further advantage of this system: with the TZT $CHCl_3$ PMMA material, fast burning in small laser spots can be achieved. This property has not been observed in any single-photon material to date mostly due to the monophotonic nature of the hole-burning process. As was demonstrated earlier for a reasonably efficient single-photon material[22], in order to detect the shallow hole burned on a ns time scale, very large reading laser spots are required to limit the reading intensity. By contrast, Fig. 6 shows that for the donor-acceptor photon-gated system, a clearly detectable spectral hole can be produced with a 30 ns pulse at λ_1 followed immediately by a 200 ms gating pulse at λ_2. The λ_1 spot diameter was 200 μm (limited by the mechanical stability of the cryostat), and the gating beam was unfocused. The 200 ms gating light pulse acts as a "developer" for centers that were placed in the lowest triplet state by the site-selecting λ_1 pulse. If many bits were to be written in the frequency domain in this material, one would simply inject short pulses at all the λ_1 wavelengths desired and then irradiate with the long λ_2 pulse to make the spectral holes permanent. This observation directly illustrates the superiority of photon-gated over single-photon mechanisms for frequency-domain optical storage applications.

One measure of the gating ratio is the inverse ratio of burning times for shallow holes of constant depth, assuming constant burning intensity at λ_1. This measure, called G_1, is approximately equivalent to the ratio of the slopes of hole growth curves for two-color versus one-color irradiation. The value of G_1 for the TZT/$CHCl_3$/PMMA system is $\simeq$ 100 at 1.5K[20]. In recent measurements, G_1 was observed to *increase* to a value near 10^4 when the temperature was raised to 20K[23]. This surprising result can be understood if the one-color hole-burning at low temperatures is due to a photophysical rearrangement of two-level systems of the nearby host polymer over shallow barriers. At higher temperatures, any one-color holes due to transitions among the same set of shallow barriers thermally erase immediately after burning. To form a detectable one-color hole at higher temperatures, much longer burning times are required because barriers must be surmounted that are large compared to kT.

Returning to Table 2, another variation of gated hole-burning material formed from the TZT molecule may be constructed by providing the halomethane acceptor as an intrinsic part of the host. Toward these ends, photon-gating has been observed for TZT in PVC (poly(vinyl chloride)) thin films[24]. However, since the effective concentration of chlorine atoms close to the TZT dopant molecules is reduced, this material shows relatively small gating ratios.

In recent studies, the group of Alshits, et al. have observed two-color photon-gating for carbazole in PMMA[25] and nonlinear one-color hole production for perylene in boric acid glass[26]. For the former system, the mechanism was determined to be N-H bond scission as was observed in previous two-photon holography experiments[27]. In the latter system, photoionization was observed upon the absorption of two quanta at 440 nm without participation of the triplet states, thus, this material may be regarded as a limiting example of 3-level photon gating shown in the left half of Fig. 2.

§4. Optimal Photon-Gating with Frequency-Domain Readout

We now turn to a discussion of the *optimal* materials parameters for practical gated recording media. In order to identify the required characteristics of a practical photon-gated storage medium, some assumptions must be made about the configuration of the frequency domain optical storage system, specifically, the detection technique used. Possible detection methods include transmission, fluorescence detection, holographic methods, electric-field readout, and time-domain readout[1]. In addition, the level of parallelism during writing and reading affects the power and time available for hole formation and detection. The configuration that has been treated in some detail that is assumed here is the case of quantum-limited transmission detection with frequency-domain readout with a single beam[28]. Some aspects of two-step spectral hole-burning with short pulses have been analyzed separately[29].

For the case of frequency domain readout, a plausible set of constraints are: 30 ns reading and writing per bit, shot-noise-limited transmission detection with at least 26 dB wideband signal-to-noise ratio, and 10 μm diameter laser spots. A useful quantity for modeling purposes is the effective hole-burning yield for photon-gated hole-burning, η_e, which is defined as the relative absorption change $\eta_e = (\Delta\alpha/\alpha)$, that is produced by the best-case two-color hole-burning during the writing time of 30 ns. Due to the complex nature of gated PSHB processes, the value of η_e depends critically on the specific microscopic properties of the gated PSHB mechanism as well as on the writing conditions.

A thorough SNR analysis for this situation[28] seeks appropriate values for the absorption cross section σ_1 at λ_1, the density of centers within a homogeneous width of the laser frequency, N_m, sample length L, and yield η_e which result in SNR $\geq$ 26 dB in a 16 MHz bandwidth. Since the values of L and N_m are not intrinsic material properties and can be controlled when fabricating the storage medium, it is helpful to classify materials by a concentration-thickness product N_mL, as long as $L \leq 100\mu m$.

Figure 7 shows the results of the analysis. Materials within the shown boundaries for particular values of η_e permit data readout with SNR equal to or greater than the required value with a maximum of 10 mW reading power. For high cross sections σ_1 and large values $N_o L$ the optical absorption becomes so strong as to prevent sufficient light from reaching the detector. For high σ_1 and low values $N_o L$ the achievable signal-to-noise is limited by power broadening of the detected holes. For $\sigma_1 \leq 10^{-15}$ cm^2 the available laser power of 10 mW is lower than the saturation power; therefore the available reading power defines the S/N limit. At the top of the figure, undesirable interactions between the optically active centers, e.g. spectral diffusion and cooperative excited-state quenching, can limit the usable concentration of centers.

As always, spectral broadening of the produced hole, either by saturation of the transition or by excessive hole-burning, imposes an upper limit on yield η_e. It is reasonable to restrict the hole-burning yield to $\eta_e \leq 0.1$. The $\sigma_1 - N_o L$ parameter space shrinks rapidly as η_e decreases. In order to successfully implement a frequency-domain optical storage system based on gated mechanisms, it is critical to find a material that permits gated PSHB with very high efficiency in the short writing times required for fast data transfer rates.

For example, with the inorganic material composed of Sm^{2+} in BaClF, $N_o L \simeq 10^{14}$ cm^{-2} and $\sigma_1 \simeq 10^{-18}$ cm^2, and the value of η_e has not been measured. The achievable SNR in this material is insufficient without more than 100 mW of reading laser power. For the case of the organic TZT/$CHCl_3$/PMMA material, $N_o L \simeq 5 \times 10^{12}$ cm^{-2}, $\sigma_1 \simeq 5 \times 10^{-12}$ cm^2, and $\eta_e \simeq 0.01$ [20]. This material would be barely acceptable if the overall efficiency were higher or if the absorption cross section were smaller (and if the mechanism were reversible).

The use of a data access method other than frequency scanning in a focused spot will clearly alter the exact materials requirements for practical information storage using photon gating. Other access methods that have been considered are time-domain storage[30], holographic storage[31], and electric-field access [32-34], and a similar SNR analysis should be performed for each of these access methods. In each case, the presence of a threshold in the

writing process improves the performance, so photon-gated materials are expected to continue to be important for information storage schemes using persistent spectral hole-burning, no matter what the access mechanism.

§5. Conclusion

The number of examples of gated spectral hole-burning continues to grow, further widening this novel class of mechanisms for PSHB. Considering the limitations on single-photon materials for frequency domain optical storage applications, the search for gated mechanisms should be an important area for future study. This is especially true because photon-gating directly resolves a paradox that limits single-photon materials: how to achieve high efficiency photochemistry for writing and yet have low efficiency during reading. The practical realization of technological applications of PSHB presents a stimulating challenge for interdisciplinary research: identification and characterization of gated hole-burning mechanisms in materials that will satisfy all the requirements for frequency domain optical storage as well as other useful applications of persistent spectral hole-burning.

ACKNOWLEDGEMENTS

The author acknowledges stimulating prior collaborations on photon-gated materials with H. W. H. Lee, M. Gehrtz, T. P. Carter, Chr. Bräuchle, and W. P. Ambrose, and the author thanks R. M. Macfarlane for permission to use Figs. 3 and 4. This research has been supported in part by the U. S. Office of Naval Research.

REFERENCES

1. See W. E. Moerner, W. Lenth, and G. C. Bjorklund: "Frequency Domain Optical Storage and Other Applications of Persistent Spectral Hole-Burning," Chapter 7 of *Persistent Spectral Hole-Burning: Science and Applications*, W. E. Moerner, editor, Topics in Current Physics Vol. 44 (Springer, Berlin, Heidelberg, 1988), and references therein.
2. W. E. Moerner: J. Molec. Elec. **1** (1985) 55.
3. See Chapters 1 through 6 of Ref. 1 for a review of many photophysical and photochemical mechanisms for persistent spectral hole-burning; also see J. Friedrich and D. Haarer: Angew. Chem. Int. Ed. Engl. **23** (1984) 113; R. Jankowiak and G. J. Small: Science **237** (1987) 618.
4. W. E. Moerner, M. D. Levenson: J. Opt. Soc. Amer. B: Optical Physics **2** (1985) 915.
5. D. M. Burland, F. Carmona, G. Castro, D. Haarer, and R. M. Macfarlane: *IBM Tech. Discl. Bull.* **21** (1979) 3770.
6. R. M. Macfarlane: J. Lumin. **38** (1987) 20.
7. As for example with dimethyl-s-tetrazine. See D. M. Burland and D. Haarer: IBM J. Res. Devel. **23** (1979) 534, and references therein.
8. A. Winnacker, R. M. Shelby, R. M. Macfarlane Opt. Lett. **10** (1985) 350.

9. A. Winnacker, R. M. Shelby, R. M. Macfarlane: J. de Phys. Colloq. C7, Suppl. 10, **46** (1985) C7-543.

10. R. M. Macfarlane, R. M. Shelby, and A. Winnacker: Phys. Rev. B **33** (1986) 4207.

11. R. J. Danby, K. Holliday, and N. Manson: J. Lumin. **42** (1988) 83.

12. C. Wei, S. Huang, and J. Yu: J. Lumin. **43** (1989) 161.

13. R. M. Macfarlane, J. C. Vial: Phys. Rev. B **34** (1986) 1.

14. A. J. Silversmith, W. Lenth, and R. M. Macfarlane: IQEC-87 Technical Digest (1987) 190.

15. H. W. H. Lee, M. Gehrtz, E. Marinero, and W. E. Moerner: Chem. Phys. Lett. **118** (1985) 611.

16. O. N. Korotaev, E. I. Donskoi, and V. I. Glyadkovskii, Opt. Spektrosk. 59 (1985) 492.

17. M. A. Iannone, G. W. Scott, D. Brinza, and D. R. Coulter: J. Chem. Phys. **85** (1986) 4863.

18. M. A. Iannone and G. W. Scott: J. Chem. Phys. **89** (1988) 2640.

19. T. P. Carter, C. Bräuchle, V. Y. Lee, M. Manavi, and W. E. Moerner: Opt. Lett. **12** (1987) 370.

20. T. P. Carter, C. Bräuchle, V. Y. Lee, and W. E. Moerner: J. Phys. Chem. **91** (1987) 3998.

21. W. E. Moerner, T. P. Carter, and C. Bräuchle: Appl. Phys. Lett. **49** (1987) 430.

22. M. Romagnoli, W. E. Moerner, F. M. Schellenberg, M. D. Levenson, and G. C. Bjorklund: J. Opt. Soc. Am. B: Optical Physics **1** (1984) 341.

23. W. P. Ambrose and W. E. Moerner: in preparation for submission to Chem. Phys. Lett.

24. T. P. Carter, W. P. Ambrose, and W. E. Moerner: unpublished results.

25. E. I. Alshits, B. M. Kharlamov, and R. I. Personov: Opt. Spectrosc. **65** (1988) 173.

26. E. I. Alshits, B. M. Kharlamov, and R. I. Personov: Opt. Spectrosc. **65** (1988) 326.

27. G. C. Bjorklund, C. Bräuchle, D. M. Burland, and D. C. Alvarez, Opt. Lett. **6** (1981) 159.

28. W. Lenth and W. E. Moerner: Opt. Commun. **58** (1986) 249.

29. I. K. Rebane: Phys. Stat. Sol. (b) **145** (1988) 749.

30. T. W. Mossberg: Opt. Lett. **7** (1982) 77.

31. A. Renn, A. J. Meixner, U. P. Wild, and F. A. Burkhalter: Chem. Phys. **93** (1985) 157.

32. G. Castro, R. H. Dicke, and D. Haarer: IBM Tech. Discl. Bull. **21** (1979) 3333.

33. U. Bogner, P. Schätz, R. Seel, and M. Maier: Chem. Phys. Lett. **102** (1983) 267.

34. U. P. Wild, S. E. Bucher, and F. A. Burkhalter: Appl. Opt. **24** (1985) 1526.

Table 1: Inorganic materials showing photon-gated persistent spectral hole-burning

Material System	λ_1, nm	λ_2, nm	Mechanism[a]	Reference
Sm^{2+} in BaClF	630,690	514-454	two-step PI	8-10
Sm^{2+} in SrClF	690	350	two-step PI	6
Sm^{2+} in CaF_2	690	514	two-step PI	6
Sm^{2+} in $CaSO_4$	690	351-514	two-step PI	11
Sm^{2+} in BaF(Cl,Br)	562	562	two-step PI	12
Co^{2+} in $LiGa_5O_8$	660	673	two-step PI	13
Cr^{3+} in $SrTiO_3$	790	790-1060	two-step PI	14

[a]PI - photoionization

Table 2: Organic materials showing photon-gated persistent spectral hole-burning

Material System[a]	λ_1, nm	λ_2, nm	Mechanism[b]	Reference
Carbazole in boric acid glass	335	360-514	two-step PI	15
Zn-TBP' in PMMA	628	337	?	16
Anthracene-tetracene photoadducts in PMMA	326	442	two-step PD	17,18
TZT with halomethanes in PMMA	630	350-800	two-step DA ET	19-21
TMT with halomethanes in PMMA	630	350-800	two-step DA ET	19,20
TZT in PVC	630	514	two-step DA ET	24
Carbazole in PMMA	337	441-514	two-step NHS	25
Perylene in boric acid glass	441	441	two-step PI	26

[a]PMMA - poly(methylmethacrylate), PVC - poly(vinyl chloride), TBP' - tetrabenzoporphyrin derivative, TZT - meso-tetra-(p-tolyl)-Zn-tetrabenzoporphyrin, TMT - meso-tetra-(p-tolyl)-Mg-tetrabenzoporphyrin.

[b]PI - photoionization, PD - photodissociation, NHS - N-H bond scission, DA ET - donor-acceptor electron transfer

FIGURE CAPTIONS

Figure 1. Illustration of basic scheme for gated, two-step PSHB. The line pointing toward "permanent reservoir" depicts the transformation of the center to a new ground state that produces hole-burning.

Figure 2. Two schemes for photon-gated PSHB. Left side: Three-level system. Right side: Four-level system. The optical absorption should be small in the circled regions.

Figure 3.. Energy level diagram of $BaClF:Sm^{2+}$ showing the two-step photoionization process responsible for photon gating.

Figure 4.. Photon gated hole-burning in the $^7F_0 \rightarrow {}^5D_0$ transition of $BaClF:Sm^{2+}$. **(a)** The 13 GHz wide inhomogeneous line profile at 6879Å, **(b)** a 700 MHz section of the line before hole-burning. **(c)** after burning at 0 MHz and -220 MHz with 2 W/cm^2 for 2000 s, **(d)** a single hole burned at 0 MHz in 3 s by adding 20 W/cm^2 of 5145Å gating light, **(e)** multiple holes burned 110 MHz apart.

Figure 5 Level diagram for photon-gated PSHB via donor-acceptor electron transfer. The structure of the donor chromophore TZT is shown in the inset.

Figure 6. Fast burning in small spots for the TZT/$CHCl_3$/PMMA material. **(a)** baseline before burning. The curvature in this trace is due to weak Fabry-Perot resonances in the

optical system. The zero of absorption is off-scale at the bottom. **(b)** After burning with a 10 mW beam at λ_1 for 30 ns, followed immediately with a 200 ms gating beam at 488 nm of 17 mW.

Figure 7. Materials constraints for gated PSHB materials in order to achieve practical SNR. The various regions and symbols are defined in the text. To illustrate the effect of increased laser power, the dotted line shows the $\eta_e = 0.1$ boundary for 100 mW reading power.

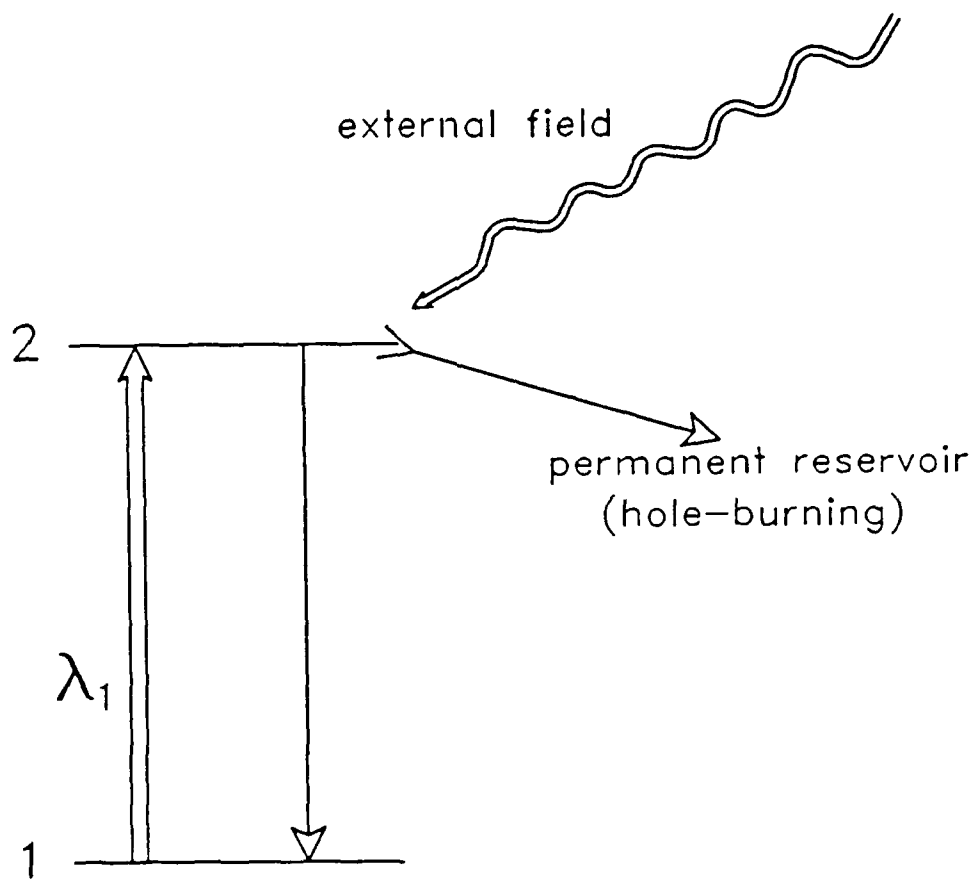
external field
2
permanent reservoir
(hole-burning)
λ_1
1

Figure 1

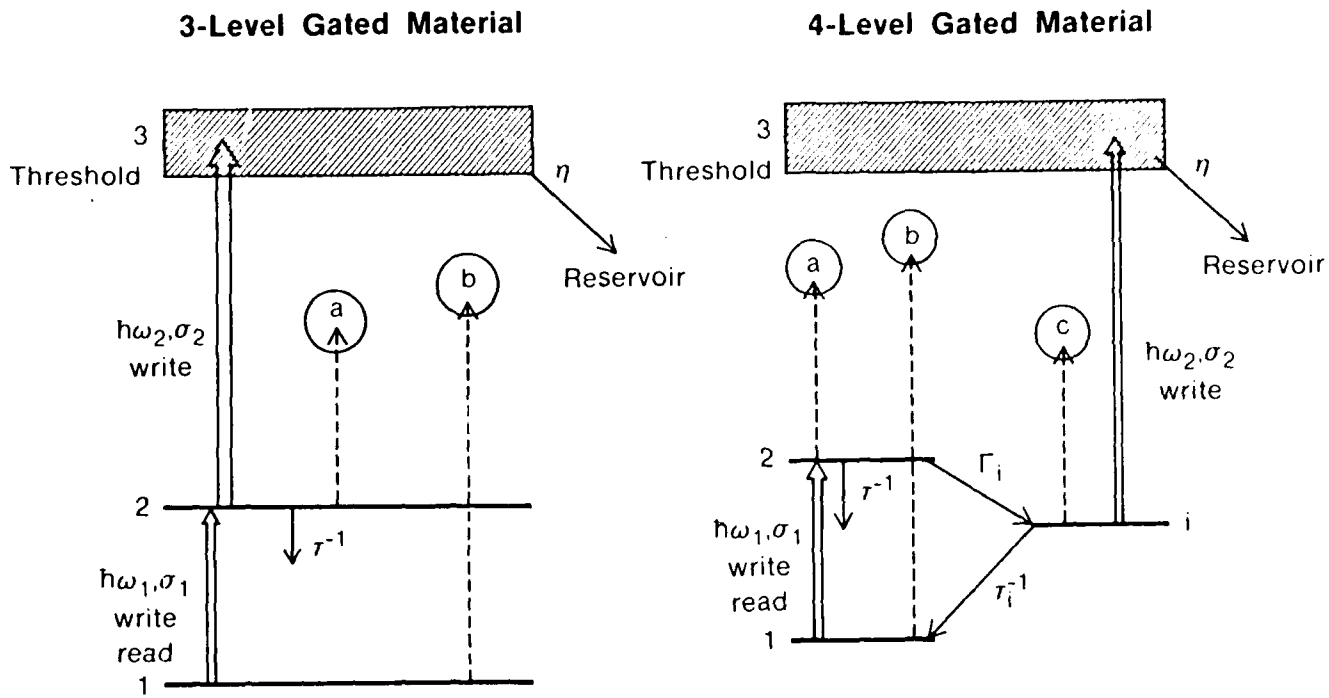
3-Level Gated Material
3
Threshold
η
Reservoir
a
b
$\hbar\omega_2,\sigma_2$
write
2
τ^{-1}
$\hbar\omega_1,\sigma_1$
write
read
1
4-Level Gated Material
3
Threshold
η
Reservoir
a
b
c
$\hbar\omega_2,\sigma_2$
write
2
Γ_i
τ^{-1}
i
$\hbar\omega_1,\sigma_1$
write
read
τ_i^{-1}
1

Figure 2

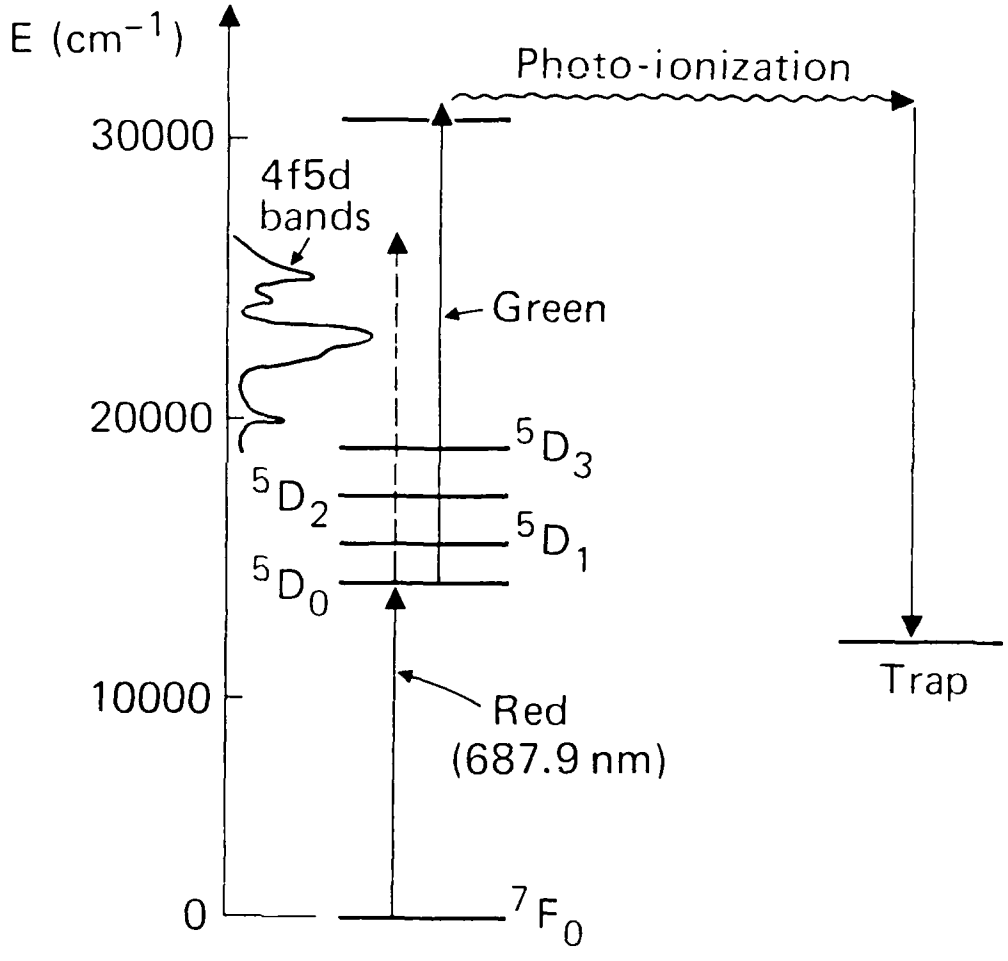
E (cm^{-1})
Photo-ionization
30000
4f5d
bands
Green
20000
$^5D_3$
$^5D_2$
$^5D_1$
$^5D_0$
Trap
10000
Red
(687.9 nm)
0
$^7F_0$

Figure 3

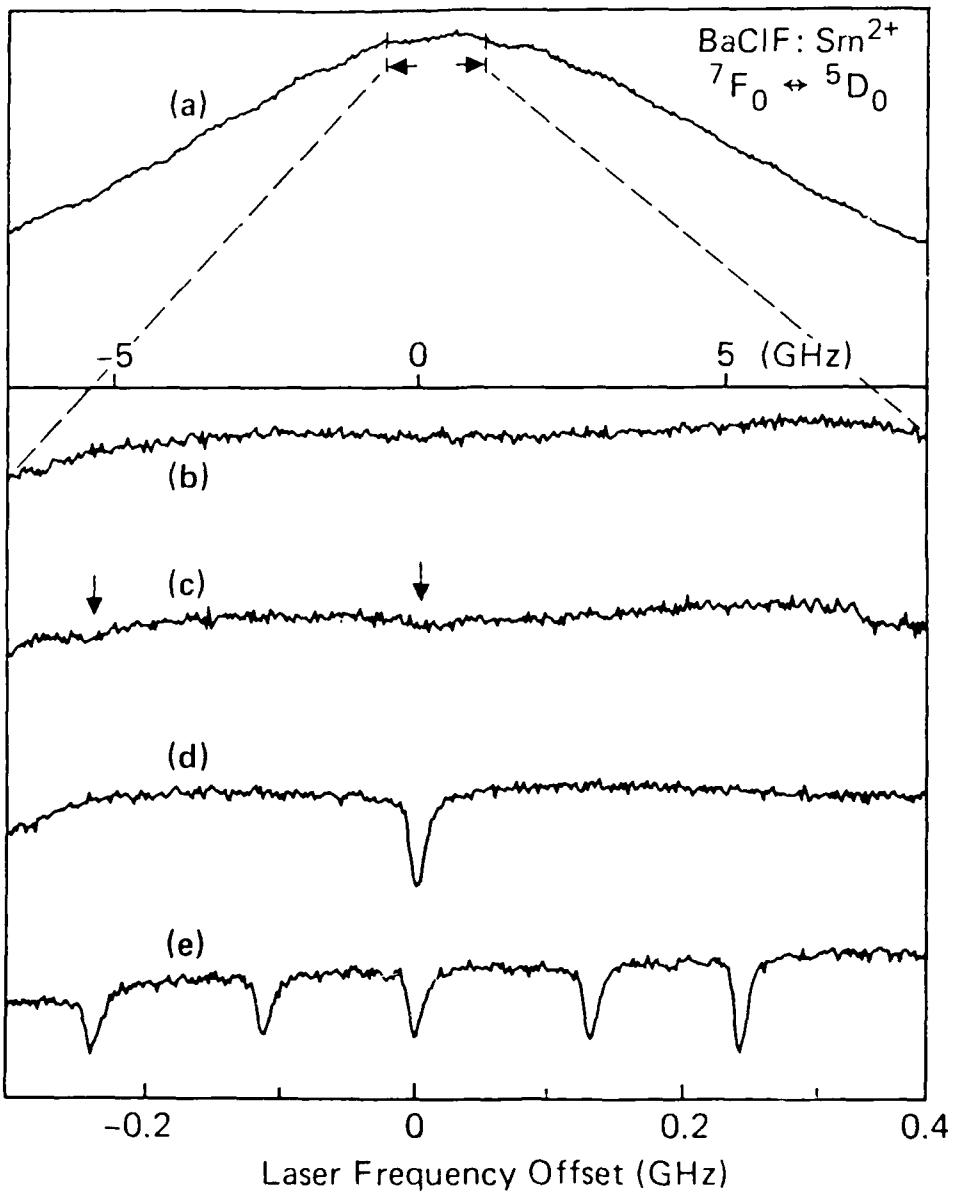
BaClF: Sm^{2+}
$^7F_0 \leftrightarrow {}^5D_0$
(a)
-5
0
5 (GHz)
(b)
(c)
(d)
(e)
-0.2
0
0.2
0.4
Laser Frequency Offset (GHz)

Figure 4

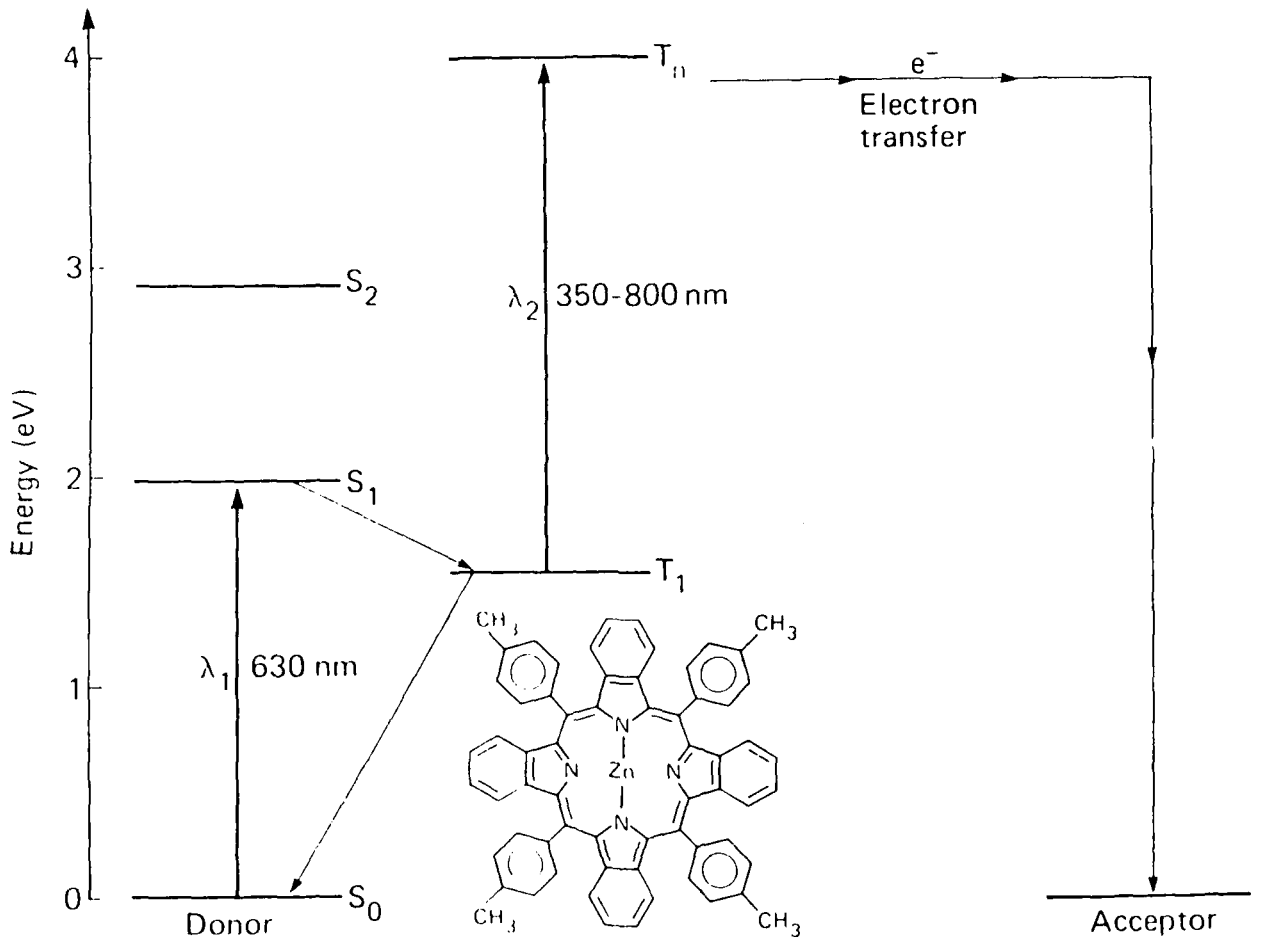
Energy (eV)
4
3
2
1
0
T_n
S_2
S_1
T_1
S_0
λ_2 350-800 nm
λ_1 630 nm
e^-
Electron transfer
Donor
Acceptor
CH_3
Zn
N

Figure 5

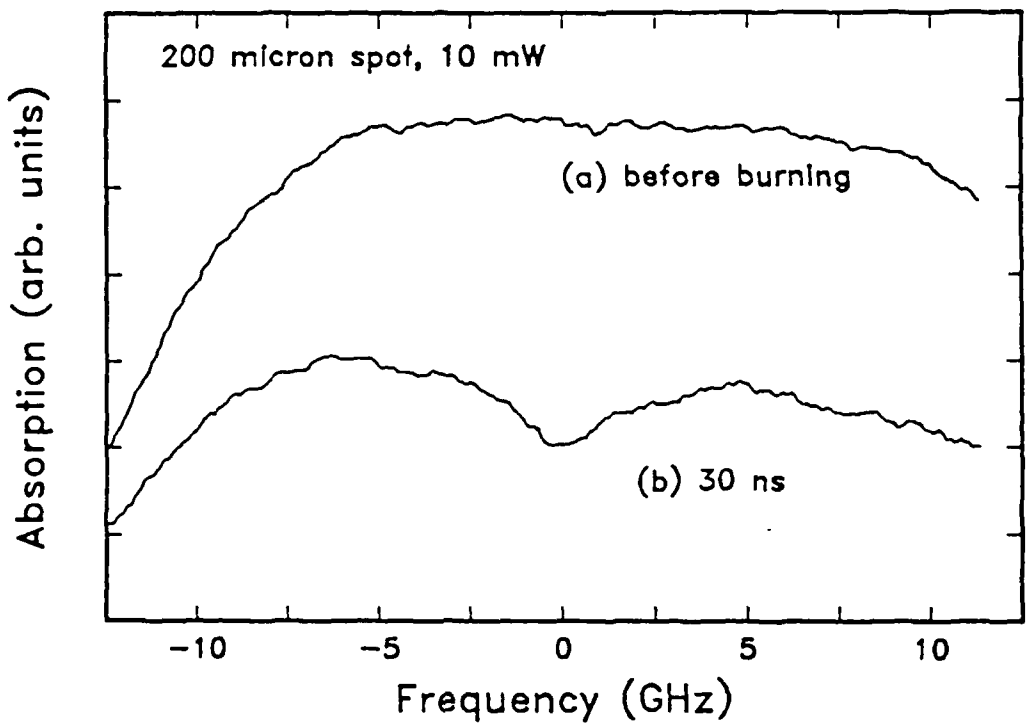
200 micron spot, 10 mW
(a) before burning
(b) 30 ns
Absorption (arb. units)
−10
−5
0
5
10
Frequency (GHz)

Figure 6

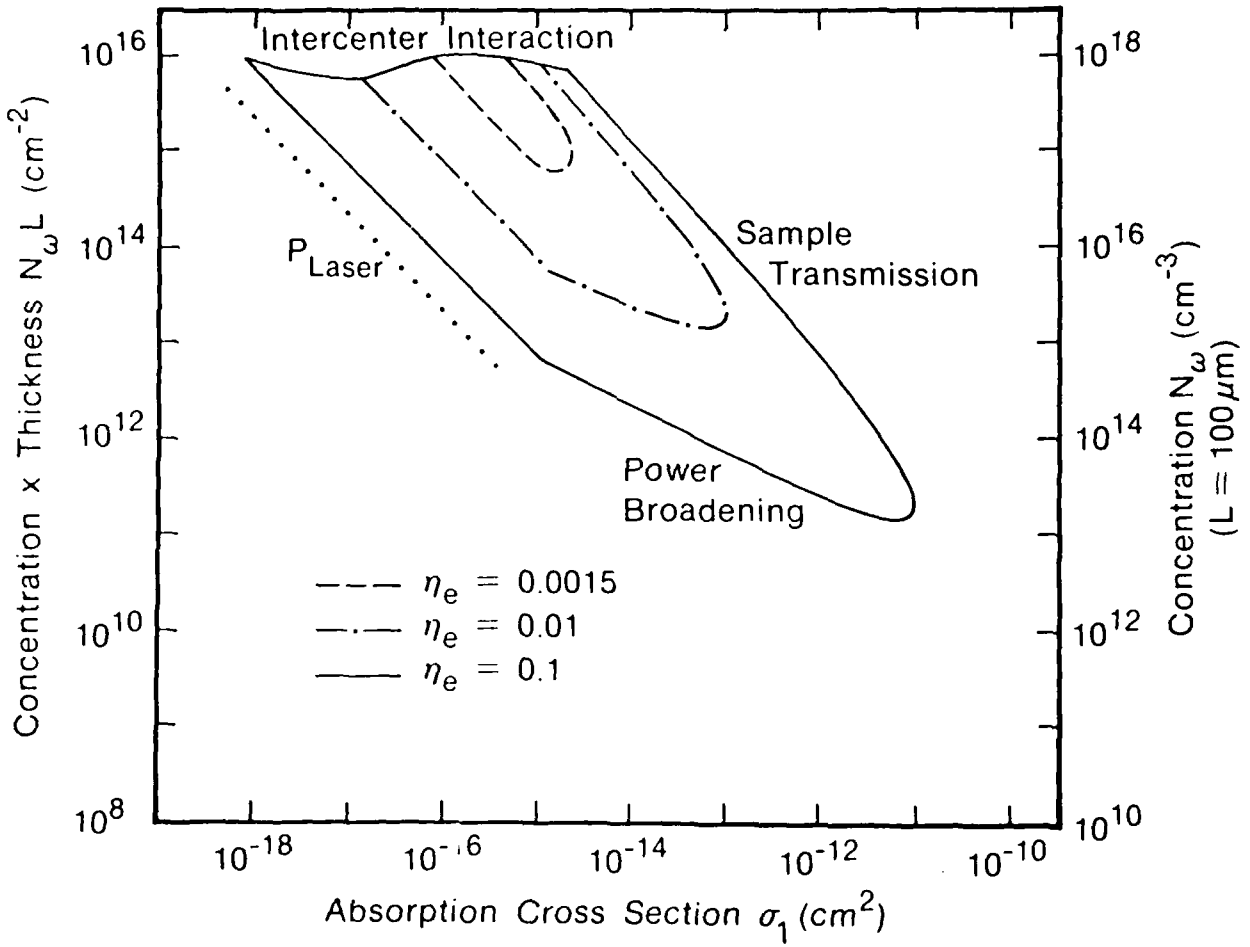
Intercenter Interaction
Sample Transmission
P_{Laser}
Power Broadening
$\eta_e = 0.0015$
$\eta_e = 0.01$
$\eta_e = 0.1$
Concentration x Thickness $N_\omega L$ (cm^{-2})
Concentration N_ω (cm^{-3}) ($L = 100\,\mu m$)
Absorption Cross Section σ_1 (cm^2)
10^{16}
10^{14}
10^{12}
10^{10}
10^{8}
10^{18}
10^{16}
10^{14}
10^{12}
10^{10}
10^{-18}
10^{-16}
10^{-14}
10^{-12}
10^{-10}

Figure 7

DL/1113/89/1

TECHNICAL REPORT DISTRIBUTION LIST, GENERAL

	No. Copies
Office of Naval Research Chemistry Division, Code 1113 800 North Quincy Street Arlington, VA 22217-5000	3
Commanding Officer Naval Weapons Support Center Attn: Dr. Bernard E. Douda Crane, IN 47522-5050	1
Dr. Richard W. Drisko Naval Civil Engineering Laboratory Code L52 Port Hueneme, California 93043	1
Defense Technical Information Center Building 5, Cameron Station Alexandria, Virginia 22314	2 high quality
David Taylor Research Center Dr. Eugene C. Fischer Annapolis, MD 21402-5067	1
Dr. James S. Murday Chemistry Division, Code 6100 Naval Research Laboratory Washington, D.C. 20375-5000	1
Dr. Ronald L. Atkins Chemistry Division (Code 385) Naval Weapons Center China Lake, CA 93555-6001	1
Chief of Naval Research Special Assistant for Marine Corps Matters Code 00MC 800 North Quincy Street Arlington, VA 22217-5000	1
Dr. Bernadette Eichinger Naval Ship Systems Engineering Station Code 053 Philadelphia Naval Base Philadelphia, PA 19112	1
Dr. Sachio Yamamoto Naval Ocean Systems Center Code 52 San Diego, CA 92152-5000	1
David Taylor Research Center Dr. Harold H. Singerman Annapolis, MD 21402-5067 ATTN: Code 283	1